Title

Cerium Tetrakis(tropolonate) and Cerium Tetrakis(acetylacetonate) Are Not Diamagnetic but Temperature-Independent Paramagnets

Journal

Inorganic Chemistry, 57(12)

ISSN

0020-1669

Authors

Halbach, Robert L
Nocton, Grégory
Booth, Corwin H
et al.

Publication Date

2018-06-18

DOI

10.1021/acs.inorgchem.8b00928

Peer reviewed

Inorganic Chemistry
Cite This: Inorg. Chem. 2018, 57, 7290−7298
Article
pubs.acs.org/IC

Cerium Tetrakis(tropolonate) and Cerium Tetrakis(acetylacetonate) Are Not Diamagnetic but Temperature-Independent Paramagnets

Robert L. Halbach,[†] Grégory Nocton,*[,†,‡,§] Corwin H. Booth,[‡] Laurent Maron,[∥] and Richard A. Andersen*[,†,‡]

[†]Department of Chemistry, University of California, Berkeley, California 94720, United States
[‡]Chemical Sciences Division, Lawrence Berkeley National Laboratory, Berkeley, California 94720, United States
[§]LCM, CNRS, Ecole Polytechnique, Université Paris Saclay, 91128 Palaiseau, France
[∥]LPCNO, UMR 5215, CNRS, INSA, UPS, Université de Toulouse, 31000 Toulouse, France

Supporting Information

ABSTRACT: A new synthesis of cerium tetrakis(tropolonate), $Ce(trop)_4$, where trop is deprotonated 2-hydroxy-2,4,6-cycloheptatrienone) or $Ce(O_2C_7H_5)_4$, is developed that results in dark-purple crystals whose X-ray crystal structure shows that the geometry of the eight-coordinate compound closely resembles a D_{2d} dodecahedron, based on shape parameters. The magnetic susceptibility as a function of the temperature (4−300 K) shows that it is a temperature-independent paramagnet, $\chi = 1.2(3) \times 10^{-4}$ emu/mol, and the L_{III}-edge X-ray absorption near-edge structure spectrum shows that the molecule is multiconfigurational, comprised of a f^1:f^0 configuration mixture in a 50:50 ratio. $Ce(acac)_4$ and $Ce(tmtaa)_2$ (where acac is acetylacetonate and $tmtaaH_2$ is tetramethyldibenzotetraaza[14]annulene) have similar physical properties, as does the solid-state compound CeO_2. The concept is advanced that $trop^-$, $acac^-$, $tmtaa^{2-}$, cot^{2-}, and O^{2-} are redox-active ligands that function as electron donors, rendering the classification of these compounds according to their oxidation numbers misleading because their magnetic susceptibilities, χ, are positive and their effective magnetic moments, μ_{eff}, lie in the range of 0.1−0.7 μ_B at 300 K.

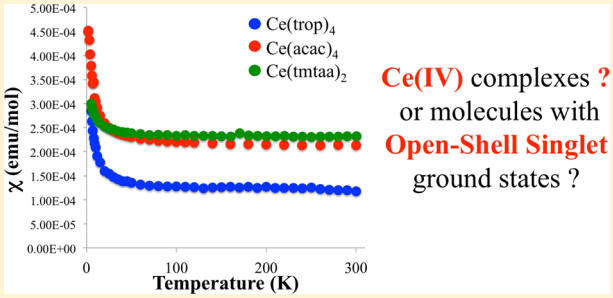

INTRODUCTION

The metal acetonylacetonate and related tropolonate compounds (Scheme 1) of the f-block metals are well-known examples of high-coordination-number polyhedra that have several applications in synthesis and spectroscopy.[1] In general, the metals in the compounds are classified according to their oxidation numbers that range from IV+ to II+, with the largest population being those of III+. The coordination geometries of the early members of the series are usually eight or higher, depending on the steric and donor effects of the ligand. Cerium presents a broad set of compounds that are classified by their oxidation numbers of IV+ and III+. The $Ce(IV,f^0)$ compounds are represented by Lewis structures in which the metal and ligands have closed-shell electron configurations, $[Ce(IV,f^0)(L^-)_4]$, and the $Ce(III,f^1)$ compounds, $[Ce(III,f^1)(L^-)_3]$, have $S = {}^1/_2$ ground states. Recent experimental and computational studies of the organometallic compound cerocene, $[Ce(\eta^8\text{-}C_8H_8)_2]$, abbreviated as $Ce(cot)_2$, show that the ground state is multiconfigurational in which the two configurations $[Ce(IV,f^0)(cot^{2-})_2]$ and $[Ce(III,f^1)(cot^{1.5-})_2]$ contribute to the ground-state wave function; see below for a brief outline of these paradigm-shifting studies. The key point is that cerocene is not represented by a single Lewis structure as implied by the empirical formula. A similar difficulty is presented by the Lewis structures of the Ce(IV) compounds of the acetylacetonate and tropolonate ligands, $[Ce(L_4)]$, which, by analogy, might be represented as $[Ce(IV,f^0)(L^-)_4]$ and $[Ce(III,f^1)(L^{3/4-})_4]$. This manuscript describes experimental and computational studies that unravel this most interesting electronic structural ambiguity.

Scheme 1. Ligands Used in This Study

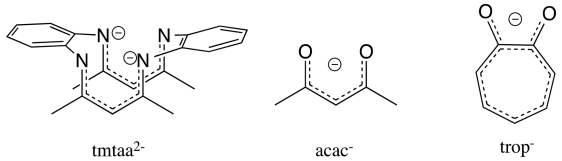

Background: Electronic Structure of Cerocene. The electronic ground state of the organometallic compound cerocene was initially thought to be a compound derived from Ce(IV), f^0, and two cyclooctatetraene dianions, $(cot^{2-})_2$ fragments, setting the valence of cerium as tetravalent. The traditional role of assigning integral values of oxidation

Received: April 9, 2018
Published: June 4, 2018

DOI: 10.1021/acs.inorgchem.8b00928
Inorg. Chem. 2018, 57, 7290−7298

numbers to metals is derived by assigning the valence of the ligands, assuming that they have a closed-shell configuration in the resulting Lewis structure. The application of these rules to $Ce(cot)_2$, and perhaps to all covalently bonded systems, is misleading because the valence of cerium is neither III+ nor IV + but is intermediate between these two integers. Early quantum-mechanical calculations,[2] followed by higher-level computational methodologies, advocated a model in which the electronic ground state is an admixture of two configurations: $[Ce(III)f^1(e_{2u})^1][(cot)^{1.5-}{}_2(e_{2u})^3]$, an open-shell singlet, and $[Ce(IV)f^0(e_{2u})^0][(cot)^{-2}{}_2(e_{2u})^4]$, a closed-shell singlet. Both configurations have the same irreducible representation of ^1A_g in D_{8h} symmetry, the point group of cerocene, and the ground state is an orbital singlet because $S = 0$. The ground-state wave function is multireference, in which the dominant one is of the form $\Psi = C_1|Ce,f^1 + (cot)_2^{1.5-}\rangle + C_2|Ce,f^0 + (cot)_2^{2-}\rangle$, where the coefficients C_1^2 and C_2^2 are approximately 80:20.[3−5] The conclusion of these articles, referred to here as the Dolg−Fulde papers, is that the Ce(III) configuration is the leading one. Two later articles, referred to as the Kerridge[6,7] papers, agree that the ground-state wave function is multireference and is $\Psi = C_1|Ce,f^1\delta,\pi e_{2u}{}^3\rangle + C_2|Ce,f^0\delta,\pi e_{2u}{}^4\rangle + C_3|Ce,f^2\delta,\pi e_{2u}{}^2\rangle$ with $C_1^2 = 0.59$, $C_2^2 = 0.23$, and $C_3^2 = 0.09$. Note that the C_1 and C_2 coefficients refer to different configurations used by the different authors. The leading configuration is the Ce(IV) configuration, which is in conflict with the earlier Dolg−Fulde calculations. This conflict is addressed in a recent paper by Mooßen and Dolg,[8] in which these authors conclude that two different interpretations of the wave functions are allowed because (i) the Kerridge model considers the molecule to be a bis(η^8-annulene[8])cerium(IV) compound with significant metal-ring covalency and (ii) the Dolg−Fulde model considers it to be a Kondo-type molecule bis(η^8-annulene[8])cerium(III) system with an atomic-like singly occupied Ce 4f shell. In a complete-active-space self-consistent-field (CASSCF) calculation, the active orbital and its associated electronic energy are not defined because they can be viewed as accidentally degenerated ones and every combination of these orbitals is a valid representation.[8] It is possible to reduce the problem to two molecular orbitals (MOs) for cerocene, namely, 4f and π^*, and for normalization purposes to define the linear combination of the two MOs as $a' = (\cos x)a + (\sin x)b$ and $b' = (\sin x)a - (\cos x)b$. If one uses, as the starting orbitals, the canonical ones, namely, the solution of the self-consistent-field (SCF) calculation on cerocene for a singlet spin state (that will be, by definition, a close-shell one), then the two MOs used are $a' = 4f$ and $b' = \pi^*$, which correspond to a x value of 25° in the expression above. This set was used by Kerridge et al. in their study, which led to an open-shell singlet ground state with a Ce(IV) leading configuration.[6,7] It should be noticed that when this choice of orbital is made, it assumes a purely ionic configuration, and the authors indicated in their discussion that they had to "turn on the covalency" by using the natural orbitals in order to obtain values that agreed with the experiment of Booth et al.[9,10] In other words, the authors needed to include mixing between the two canonical MOs in order to obtain results in line with the experiments. In the approach of Dolg, however, this mixing is intrinsically included in the expression of the a' and b' MOs. In his seminal work, Dolg reported $a' = 0.8(4f) + 0.2\pi^*$ and $b' = 0.2(4f) + 0.8\pi^*$ (which correspond to $x = 17.5°$) and a wave function that was 80% Ce(III) and 20% Ce(IV), in line with Booth's experimental results. Despite the apparent discrepancy between the two results, both of them can be considered valid because, as mentioned earlier, whatever linear combination of the MOs that is used in the CASSCF calculation, only a comparison with the experiment gives insight into the valid choice. Dolg's approach may be considered simpler because it is based on only two MOs. However, the number of possible linear combinations is infinite, and neither one of the two approaches can be viewed as the ultimate one.

The important point that emerges from the different calculations is that the ground-state wave function is multireference and multiconfigurational and cannot be described by a single Lewis structure. The magnetic susceptibility showed that Ce in cerocene is not diamagnetic because χ demonstrates temperature-independent paramagnetism (TIP) to 300 K, resulting from thermal mixing between the ground state with the excited triplet state by the Boltzmann factor.

The computational models erase the conceptual difficulty that a strongly oxidizing metal, Ce(IV), coexists with a ligand that is strongly reducing because the net result of the intramolecular electron transfer develops a multiconfigurational ground state and the compound follows Pauling's electroneutrality principle, and that cot^{2-} is a net electron donor.

Experimental studies of the magnetic properties of $Ce(cot)_2$ and the L_{III}-edge X-ray absorption near-edge-structure (XANES) spectroscopy as a function of the temperature showed that the magnetic susceptibility and the f^1/f^0 signatures are independent of the temperature from 30 to 300 K. The value of n_f, deduced from the XANES spectra, C_1^2, is approximately 0.8,[9−11] in agreement with the quantum-mechanical model advocated by the Dolg−Fulde papers.[9−11] Magnetic and spectroscopic studies on formally tetravalent cerium organometallic compounds bis(hexamethylpentalene) cerium and the bis(triisopropylsilyl) analogue show that they also have multiconfigurational ground states in which cerium is intermediate valent.[12,13] The photoelectron spectra of Cp_3Ce suggest that the cation state, $Cp_3Ce^+(g)$, is multiconfigurational.[14] Thus, the multireference model seems to be widely applicable to those organometallic compounds in which the electrons in filled π-bonding orbitals on the ligands function as electron donors to empty orbitals on the metal, as in cerocene and Cp_3Yb,[15] and those in which the empty π orbitals are acceptor orbitals, as in $Cp^*_2Yb(bipy)$ and related compounds.[16−22]

A question that arises naturally is, can nonorganometallic ligands used in traditional coordination compounds of formally tetravalent cerium also function as electron donors, resulting in compounds with multiconfigurational ground states? The L_{III}-edge XANES spectra of several phthanocyanine and phorphyrin compounds of formally Ce(IV) have f^0/f^1 signatures,[23,24] implying that they are multiconfigurational. The variable-temperature magnetic susceptibility of tetraazamacrocycle[14]-annulene cerium, $Ce(tmtaa)_2$, is independent of the temperature, indicative of a nonmagnetic ground state, but the "Ce(IV)" compound was not studied in greater detail.[25]

This Article reports experimental and computational studies on $Ce(tmtaa)_2$, $Ce(acac)_4$, and $Ce(trop)_4$, where acac and trop are abbreviations for the deprotonated ligands of 2,4-pentanedione and 2-hydroxy-2,4,6-cycloheptatrienone, respectively (Scheme 1). These studies show that the ground states are open-shell singlets that have populated open-shell triplet excited states, resulting in TIP magnetic behavior. These molecular compounds have physical properties that are related

DOI: 10.1021/acs.inorgchem.8b00928
Inorg. Chem. 2018, 57, 7290−7298

to those of the solid-state material CeO_2, implying that they have similar electronic structures.

RESULTS AND DISCUSSION

Synthesis. The original synthesis of $Ce(trop)_4$ was by the addition of 2-hydroxy-2,4,6-cycloheptatrienone (tropolone) to ceric ammonium nitrate in aqueous acidic methanol,[26] and it was described as a "black crystalline material" from dichloromethane. A new synthesis is developed by the addition of a slight excess of tropolone, $pK_a = 6.7$[27] in water, to a toluene solution of $Ce(acac)_4$ (the pK_a value of acacH is 9 in water;[28] eq 1).

$$Ce(acac)_4 + 4tropH \rightarrow Ce(trop)_4 + 4acacH \quad (1)$$

The dark precipitate that forms immediately is purified by Soxhlet extraction with chloroform in air. The dark-purple crystals are insoluble in hydrocarbon solvents and sparingly soluble in chlorinated hydrocarbons. The crystals appear black to the naked eye but yellow-orange in a dilute solution of CH_2Cl_2 because of a broad absorption at approximately 450 nm ($\varepsilon \approx 2000\ M^{-1}$); the ultraviolet absorptions are listed in the Experimental Section. An absorption around 500 nm is assigned to ligand-to-metal charge transfer in cerirum tetrakis-(pyridylnitroxide) complexes.[29−31] The ^{1}H NMR spectrum in $CDCl_3$ at 20 °C consists of a triplet at 7.44 ppm, $J = 9.6$ Hz, a doublet at 7.08 ppm, $J = 10.4$ Hz, and a triplet at 6.90 ppm, $J = 9.6$ Hz, in an area ratio of 8:8:4, assigned to Hβ, Hα, and Hγ, respectively. The ^{1}H NMR spectrum at 20 °C indicates an average stereochemistry in solution because site exchange is often rapid in eight coordination, but the spectrum is a useful indicator of purity. The ^{1}H NMR resonances are slightly broadened, which is apparent upon a comparison of the resonances due to Hγ in the complex and free tropolone. In the free ligand, Hγ appears as a triplet of triplets centered at $\delta_H = 6.97$ with $^3J_{H\gamma H\beta} = 9.0$ Hz and $^4J_{H\gamma H\beta} = 1.2$ Hz; in the complex $\delta\gamma = 6.90$ ppm is a triplet with $^3J_{H\gamma H\beta} = 9.6$ Hz and $^4J_{H\gamma H\beta}$ is not resolved within the line width. There is no exchange between these resonances on the NMR time scale when a small amount of tropolone is added.

X-ray Crystal Structure. The compound $Ce(trop)_4(tropH)$ crystallizes in the monoclinic crystal system in space group $C2/c$, and an ORTEP is shown in Figure 1; the free tropolone present in the unit cell is not shown in Figure 1, but its location is shown in a packing diagram available in the Supporting Information (SI). The crystal used was obtained by dissolving the solid, obtained from the reaction indicated in eq 1, in a mixture of $CHCl_3$ and toluene (5:1) and allowing the solution to slowly evaporate; small dark-purple crystals formed over a few days. The crystal data are available in the Experimental Section, and all bond distances and angles are available in the SI.

The average Ce−O distance in $Ce(trop)_4$ is 2.354 ± 0.010 Å with a range of 2.336(2)−2.388(2) Å. The average Ce−O distances in $Ce(acac)_4$ and related derivatives are available in the CCDC range from 2.31 to 2.39 Å with an average distance of 2.33 Å (Table 1). The Ce−O distance in $Ce(trop)_4$ is slightly longer than the equivalent distances in the acetylacetonate derivatives but within the range observed. These Ce−O distances are significantly longer than the Ce−O distance found in the tetrakis(pyridylnitroxide) complexes reported recently that lie between 2.2 and 2.23 Å.[30,31] The geometry of $Ce(trop)_4$ is close to an idealized D_{2d}

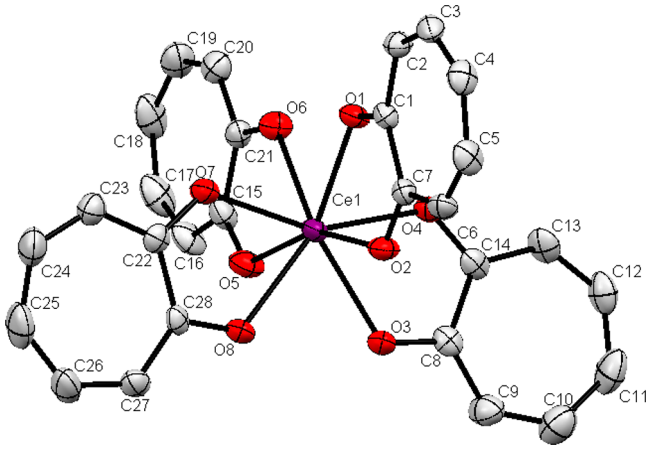

Figure 1. ORTEP of $Ce(trop)_4(tropH)$, with 50% probability ellipsoids. The non-H atoms are refined anisotropically, and the H atoms are placed in ideal positions and are not refined. The cocrystallized tropH molecule is not shown; see the SI.

Table 1. Average Ce−O Distances in $Ce(acac)_4$ and Related Derivatives Available in the CCDC

R	R′	Ce−O(ave)	ref
Me	Me	2.39 ± 0.02	*a*
Me	Me	2.32 ± 0.03	*b*
Me	Me	2.33 ± 0.02	*c*
Me	Me	2.33 ± 0.02	*d*
CMe_3	CF_3	2.32 ± 0.04	*e*
CH_2CHMe_2	Ph	2.33 ± 0.04	*f*
Me	Ph	2.34 ± 0.02	*g*
CMe_3	CMe_3	2.31 ± 0.02	*h*
		2.32 ± 0.02	
CF_3	CF_3	2.34 ± 0.01	*i*
CMe_3	$CHMe_2$	2.31 ± 0.03	*j*
		2.32 ± 0.04	
		2.32 ± 0.02	
Ph	Ph	2.32 ± 0.02	*k*
CMe_3	$C(OMe)Me_2$	2.32 ± 0.02	*l*

[a]Reference 32. [b]Reference 33. [c]Reference 34. [d]Reference 35. Both the α and decahydrate $Ce(acac)_4$ complexes are reported. Line d reports the metrics for the decahydrate $Ce(acac)_4$ complex. [e]Reference 36. [f]Reference 37. [g]Reference 38. [h]Reference 39. [i]Reference 40. [j]Reference 41. [k]Reference 42. [l]Reference 43.

dodecahedron, as shown by the shape parameters in Table 2 (Figure 2).

Several crystal structures of neutral and anionic eight-coordinate metal tropolonate compounds are known, and their geometries generally are closer to that of a dodecahedron (D_{2d}) than to that of a bicapped trigonal prism when the shape parameters are used to make this distinction. The geometries of the lanthanide anions $[M(trop)_4]^-$ from Tb to Lu are close to dodecahedral,[44] as are the neutral $M(trop)_4$, M = Zr, Hf.[45−47] The anion $[Sc(trop)_4]^-$ and cation $[Nb(trop)_4]^+$ are described as bicapped trigonal prisms distorted toward a dodecahedron.[48,49]

Variable-Temperature Magnetic Susceptibility, χ, and L_{III}-Edge XANES Spectroscopy. The sample used for solid-state magnetic susceptibility of $Ce(trop)_4$ was obtained by Soxhlet extraction in and crystallization from $CHCl_3$ and shown to be free from cocrystallized tropolone by ^{1}H NMR spectroscopy and combustion analysis. The plot for $Ce(trop)_4$

DOI: 10.1021/acs.inorgchem.8b00928
Inorg. Chem. 2018, 57, 7290−7298

Table 2. Shape Parameters for Eight-Coordinate Compounds[50]

compound	δ_1	δ_2	δ_3	δ_4	ϕ_1	ϕ_2	ref
$Ce(trop)_4$	31.5	31.8	33.3	36.1	0.90	1.77	this work
α-$Ce(acac)_4$	9.7	21.1	44.0	42.9	12.8	15.3	*b*
β-$Ce(acac)_4$	5.3	5.3	46.7	46.7	19.7	19.3	*b*
$Ce(tmtaa)_2$	0.83	1.12	1.14	1.45	0.24	0.59	this work
$Ce(nitroxide)_4$	30.7	30.9	49.0	49.5	7.8	11.0	*a*
$Zr(trop)_4$	22.9	31.8	32.4	40.1	6.6	1.9	*d*
$Hf(trop)_4$							*e*
$Sc(trop)_4^-$	13.4	29.0	42.3	43.0	10.8	10.8	*f*
$Nb(trop)_4^+$	19.4	21.0	42.9	45.1	11.5	13.9	*g*
D_{2d} dodecahedron	29.5	29.5	29.5	29.5	0	0	
square antiprism	0	0	52.4	52.4	24.5	24.5	
square prism	0	0	0	0	0	0	
bicapped trigonal prism	0	21.8	48.2	48.2	14.1	14.1	

[a]Reference 31. [b]Reference 51. [c]Reference 25. [d]Reference 45. [e]Reference 46. [f]Reference 48. [g]Reference 52.

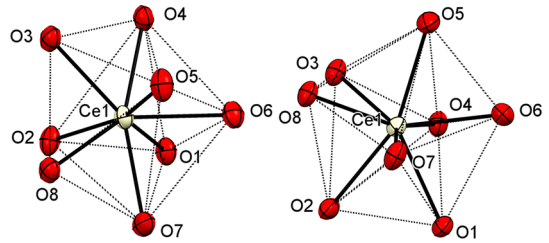

Figure 2. Two views of the coordination polyhedron of $Ce(trop)_4$ showing the planes used to calculate the shape parameters.

of χ versus T is shown in Figure 3, and similar plots for $Ce(acac)_4$, $Ce(tmtaa)_2$,[25] and the solid-state compound CeO_2

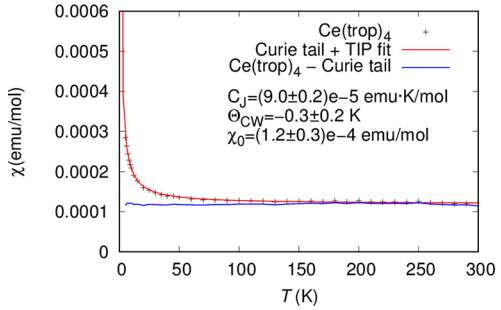

Figure 3. Magnetic susceptibility data for the complex $Ce(trop)_4$. The value of $\chi_0 = (1.2 \pm 0.3) \times 10^{-4}$ emu/mol is corrected for residual diamagnetism using Pascal's constants and for a small amount of magnetic impurity.

are shown in Figure 4. The cerium contribution to the susceptibility is isolated by subtracting the other contributions from the complex using Pascal's constants, and each data set is subsequently fit to a conventional Curie–Weiss model with $\chi = C_J/(T - \Theta_{CW}) + \chi_0$, where C_J is known as the Curie constant, Θ_{CW} is the Curie–Weiss temperature and indicates the strength of magnetic interactions, and χ_0 indicates the magnitude of the temperature-independent component. The small values of C_J are consistent with a paramagnetic impurity corresponding to less than 0.2% of a Ce(III) impurity in all cases. All data were collected at two applied fields to account for any ferromagnetic impurity in the container, and these correspond to less than 0.15% of Fe in all cases.

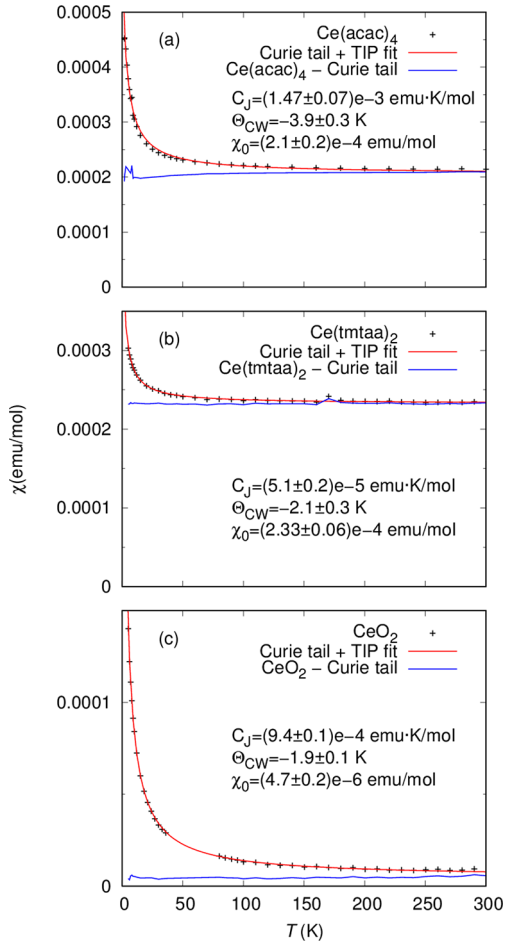

Figure 4. Magnetic susceptibility data for the compounds (a) $Ce(acac)_4$, (b) $Ce(tmtaa)_2$, and (c) CeO_2. The values reported in the legends and Table 3 of χ_0 are corrected for residual diamagnetism using Pascal's constants and for a small amount of magnetic impurity.

The plots of χ versus T for all of these compounds show that, after the diamagnetic correction for the ligand, χ is positive and, after fitting for a small paramagnetic impurity, independent of the temperature from 5 to 300 K; none of the cerium in these "Ce(IV)" molecules and the solid-state CeO_2 material is diamagnetic (i.e., χ is not negative), but they are temperature-independent paramagnets, implying that the excited state (ot) is close in energy to the ground state that is an open-shell

DOI: 10.1021/acs.inorgchem.8b00928
Inorg. Chem. 2018, 57, 7290–7298

singlet (os). If the cerium in these compounds were diamagnetic, $\chi < 0$, then their electronic ground states would be closed-shell singlets, $S = 0$ and $L = 0$, and their Lewis structures would be represented as $[Ce(IV,f^0)(L^{-1})_4]$, in which the f-orbital population is zero and each ligand is closed-shell and a monoanion. This classical representation results when molecules are classified by the oxidation number formalism, a classification that is misleading for $Ce(trop)_4$ and the related molecules mentioned above and may well be misleading for other reported high-oxidation-number lanthanide compounds.

The XANES spectra reflect the trends shown in the magnetic susceptibility measurements. As can be seen in Figure 5, the Ce

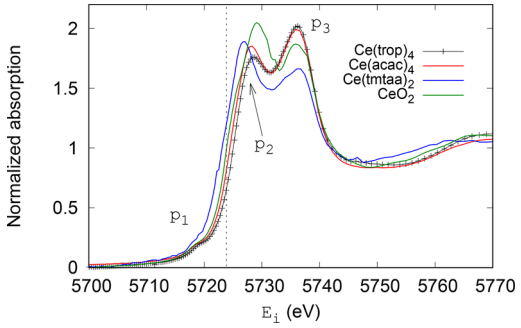

Figure 5. Ce L_{III}-edge XANES spectra for $Ce(trop)_4$ compared to the spectra from $Ce(acac)_4$, $Ce(tmtaa)_2$, and CeO_2. The vertical dotted line shows the position for a Ce(III) compound, $Ce[N(Si(CH_3)_3)_2]_3$, from ref 9. The labels are described in the text.

L_{III}-edge absorption data include a small peak (p_1) just below 5720 eV associated with a direct $2p_{3/2} \rightarrow 4f$ transition,[53] followed by an initial excitation starting near 5710 eV and then by two main peaks (p_2 and p_3), one just below 5730 eV and another at about 5736 eV. Peak 3 is associated with the ionic-like Ce(IV) contribution to the ground state. Peak 2 reflects the f^1 contribution to the ground state, be it ionic or reflecting ligand charge transfer to the Ce, that is, an f^1 configuration or an $f^1\underline{L}$ configuration. The latter configuration is typical of a covalent bond, and the ensuing delocalization of the f electron can reduce the core–hole screening effect of that electron on the outgoing photoelectron, with the effect that a more delocalized f electron will cause an upward energy shift of that peak (e_2). This shift is clear from the position of an ionic Ce(III) spectrum, as indicated by the dotted line in Figure 5. The overall f occupancy, n_f, is determined as the relative weight (area) of peak 2 to the total weight of peak 3. This value can also be thought of as the degree of covalency in the Ce bonds in the compound.[54]

It is important to note that weak and/or unresolved features, likely resulting from crystal-field effects, are obscured by the main peaks in these spectra. These features are better resolved using higher-resolution techniques, such as high-energy-resolution fluorescence detection (HERFD).[53] Despite the limitations of the simple double-peak model described above, our approach remains reasonably accurate because the splitting of the states is on the order of the core–hole lifetime of the $2p_{3/2}$ hole.[55]

Given this background, these data were fitted with a combination of a steplike function, Gaussians to model the aforementioned peaks, and a Gaussian to roughly account for the first negative EXAFS oscillation near 5750 eV. More fitting details and results are presented in the SI, but the main results are summarized in Table 3. Trends in χ_0 are reflected in the n_f for the molecules studied, as are trends in e_2, with the most delocalized (highest e_2) value corresponding to the lowest n_f and χ_0. Also presented are the data for CeO_2 as a canonical formally tetravalent Ce system. In this case, although it has a somewhat high value of n_f, e_2 is high, consistent with a strongly covalent system, and although this extended solid should not be quantitatively compared to the other molecules studied here, the high value of e^2 is also consistent with the low value of χ_0.

Calculations. The calculations are all CASSCF/CAS-SDCI methodologies. Four electrons were distributed over five orbitals (four atomic 4f orbitals and the ligand lowest low-lying orbital). Then, as was already done for calculations on $Cp^*_2Yb(bipy)$, the number of active electrons was reduced to two and compared to the results obtained with a larger number of active electrons. The results were found to be consistent. The choice of the starting orbitals was also carefully investigated by trying several sets of MOs. MOs arising from either the f^1L^7 or f^0L^8 SCF calculations were considered, where the term f^1L^7 or f^0L^8 refers to a generic term to describe symmetry-adapted ligand orbitals (mainly O p lone pairs). In both cases, the T1 diagnostic of the CASSCF was found to be too large, although smaller for the first choice than the second one, indicating that the MOs were not optimal to describe the states. This was due to implication of the f^2 states, although to a small amount, in the wave function. Therefore, averaged orbitals arising from the two states (f^1L^7 and f^0L^8) were considered. Although T1 was reduced, it was still too high, indicating the need to describe the f^2 states. Thus, the final set of MOs used in this study were obtained by averaging the MOs of the three states, f^2L^6, f^1L^7, and f^0L^8, using different weights (5,47,48 and 33,33,33). Both sets yielded the same results, described in this contribution. Finally, by the fact that T1 was still large, configuration interaction (CI) calculations were carried out on top of the CASSCF. Because single and double excitations were taken into account, the MOs were improved during the CI calculation.

Table 3. Magnetic and L_{III}-Edge XANES Data and Calculated Energies between the Different States (cs, Closed-Shell Singlet; os, Open-Shell Singlet; ot, Open-Shell Triplet)[a]

compound	χ (emu/mol)	n_f	e^2	e^3	E(os-ot)[b]	E(os-cs)[b]	μ_{eff} (μ_B,300 K)
$Ce(trop)_4$	1.2(3)x10^{-4}	0.50(3)	5728.2(3)	5736.0(3)	0.009 (73)	0.059 (476)	0.54(7)
$Ce(acac)_4$	2.1(2)x10^{-4}	0.51(3)	5727.9(3)	5735.9(3)	0.005 (40)	0.065 (523)	0.71(4)
$Ce(tmtaa)_2$	2.33(6)x10^{-4}	0.59(3)	5726.8(3)	5735.6(3)	0.008 (65)	0.088 (710)	0.75(1)
CeO_2	4.7(2)x10^{-6}	0.58(3)	5728.2(3)	5736.5(3)			0.106(2)
Cerocene	1.4(2)x10^{-4}	0.82(3)	5725.0(3)	5736.5(3)			0.58(4)

[a]The standard deviation in the last digit is reported in parentheses for each measurement. Absolute errors are reported for n_f, e^2, and e^3. The relative error is smaller, about unity in the last reported digit. The effective moment at 300 K, μ_{eff}, is calculated from χ_0. [b]In eV (cm^{-1}).

DOI: 10.1021/acs.inorgchem.8b00928
Inorg. Chem. 2018, 57, 7290–7298

The four possible states that define the electronic states in which two electrons, one a cerium 4f electron and the other a ligand-based electron, can be distributed as indicated in Scheme 2. The energy scale is arbitrary.

Scheme 2. General Energy Diagram of the Different Configurations Discussed in This Article

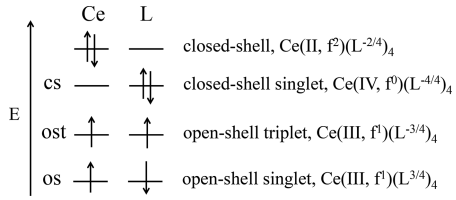

The calculations show that the ground-state configuration of the three inorganic coordination compounds is an open-shell singlet, os. In each of the compounds, the triplet state, ot, is nearly degenerate but lies slightly higher in energy than the open-shell singlet. Besides the f^2 configuration, the closed-shell singlet, f^0, configuration is highest in energy in all three compounds. The relative energies in the three compounds and configurations that contribute to the ground-state wave function are illustrated in Scheme 3.

The calculated values of n_f, the number of f electrons in the initial electronic ground state, which is equal to C_2^2 in the wave function $\Psi = C_1|\mathrm{Ce(IV,4f^0)}(L - L^{-1})_4\rangle + C_2|\mathrm{Ce(III,4f^1)}(L - L^{-3/4})_4\rangle$, are in good agreement with the experimental value of n_f [0.42 vs 0.50 for $Ce(trop)_4$; 0.48 vs 0.51 for $Ce(acac)_4$; 0.41 vs 0.59 for $Ce(trop)_4$]. They indicate that the f^1 contribution to the wave function is about 50%, not zero for a closed-shell configuration. The value of C_2^2 in the wave function depends slightly on the ligand in the order acac > trop ≈ tmtaa, while the value of n_f is tmtaa > acac ≈ trop. The role the ligand plays in determining the coefficient of the f^1 configuration more or less follows the electronegativity of the ligating atoms in the three 16-electron coordination compounds and the 20-electron organometallic compound, C > N > O; therefore, COT ≫ tmtaa > acac ≈ trop (using the experimental values). Accordingly, the general order of sharing of the ligand-localized electron with the appropriate empty symmetry orbitals localized on cerium is related to the relative energy separation between the ligand highest occupied molecular orbital (HOMO) and cerium lowest unoccupied molecular orbital (LUMO) energies: the closer the energies, the larger the amount of sharing of the ligand electrons with the metal orbitals.

The small-calculated separation between os and ot is responsible for the TIP behavior observed experimentally and the small net value of μ_{eff} because the os ($S = 0$) mixes with the ot in an applied magnetic field and the population depends on the Boltzmann factor.

SUMMARY

The new synthesis of $Ce(trop)_4$ exploits the relative pK_a values of tropolone and acethylacetone and promises to be a useful and general synthetic method for the preparation of other metal tropolonate compounds because the metal acetylacetonates are usually easily prepared and soluble in hydrocarbon solvents for most of the metals and nonmetals in the periodic table, provided that they are kinetically labile.

The key point that emerges from the experimental study of the four isoelectronic molecules of cerium is that cerium is not diamagnetic in any of them because $\chi > 0$ and magnetically they behave as temperature-independent paramagnets. The wave function based on computational methods provides an explanation for the TIP; i.e., the small difference in energy between the open-shell singlet ground state and the open-shell triplet first excited state ranges from 40 to 75 cm^{-1}, allowing for Van Vleck paramagnetism.[56,57]

The energy of the open-shell singlet that corresponds to the traditional Lewis structures used to represent these molecules is 400−700 cm^{-1} above the open-shell triplet. A general MO diagram for these molecules is inappropriate for these 16-electron molecules because of their different point groups, highlighting the difficulties in understanding the difference between a Lewis structure represented by a single-reference wave function and the open-shell singlet multireference wave function.

Electronic Structure of CeO_2 from the Molecules. The solid-state material, CeO_2, plays an important role in catalysis because it can function as an O-atom donor in oxidation reactions or as a H-atom-transfer catalyst in hydrogenation reactions. CeO_2 is an insulator with a band gap of 6.0 eV, but its ground-state electronic structure is controversial.[58] The measured magnetic susceptibility between 5 and 300 K of CeO_2 (Figure 5) features TIP behavior, and the L_{III}-edge XANES spectra also have signatures of both f^0 and f^1 contributions (Figure 5). From the model discussed herein

Scheme 3. Energy Diagram of the Configuration-Calculated States for $Ce(trop)_4$, $Ce(acac)_4$, and $Ce(tmtaa)_2$

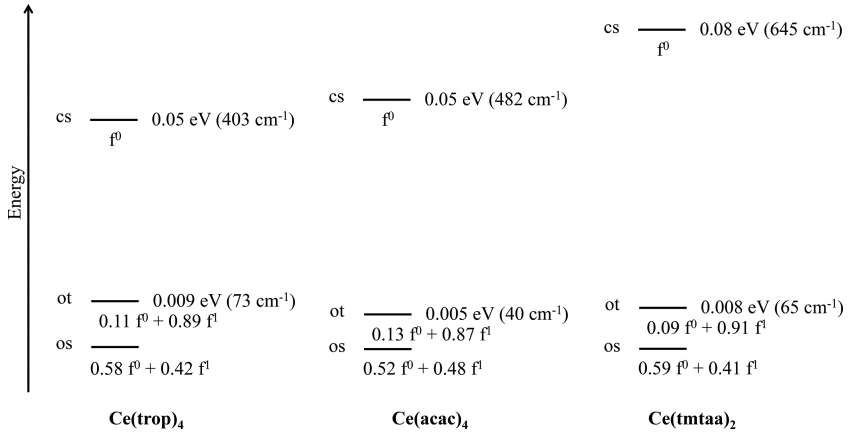

DOI: 10.1021/acs.inorgchem.8b00928
Inorg. Chem. 2018, 57, 7290−7298

for coordination molecules, it seems that CeO_2 would fall in the same category. Thus, these molecules would provide a deeper level of understanding of the electronic structure and chemical and physical properties of the solid-state material CeO_2, a further important step.

EPILOGUE

The electronic structures of four molecules, $Ce(cot)_2$, $Ce(acac)_4$, $Ce(trop)_4$, and $Ce(tmataa)_2$, have similar L_{III}-edge XANES features attributed to both Ce(IV,f^0) and Ce(III,f^1) and magnetic susceptibility plots showing that the molecules are temperature-independent paramagnets to 300 K. The similarity of the spectroscopic features of the molecules and CeO_2 shows that they have similar electronic structures. CASSCF calculations on the molecules show that the ground state is an open-shell singlet with an n_f of about 0.5 and the first excited state is an open-shell triplet that is close in energy. These two states are populated, resulting in TIP behavior. The notion that Lewis structures, which are traditionally written for the set of cerium coordination and organometallic compounds, are misleading, indeed wrong, should surprise the readers of this Article. The magnetic and spectroscopic measurements coupled with multireference wave-function-based methodologies that are required to develop the new model are laborious and time-consuming but rewarding.

EXPERIMENTAL SECTION

General Considerations. All reactions were performed using standard Schlenk-line techniques or in a drybox (MBraun). All glassware was dried at 150 °C for at least 12 h prior to use. Toluene and pentane were dried over sodium and distilled, while CH_2Cl_2 and $CHCl_3$ were purified by passage through a column of activated alumina. Toluene-d_8 was dried over sodium, and $CDCl_3$ was used as purchased from Aldrich. All of the solvents were degassed prior to use. Tropolone was purified by sublimation in a vacuum, and $Ce(acac)_4$ was prepared by a literature method.[59]

^{1}H NMR spectra were recorded on Bruker AVB-400 MHz and Advance 300 MHz spectrometers. ^{1}H chemical shifts are in δ units relative to tetramethylsilane, and coupling constants (J) are given in hertz. IR spectra were recorded as Nujol mulls between KBr plates on a Thermo Scientific Nicolet IS10 spectrometer. Samples for UV−vis−near-IR spectroscopy were obtained in a Schlenk-adapted quartz cuvette and obtained on a Varian Cary 50 scanning spectrometer. Melting points were determined in sealed capillaries prepared under nitrogen and are uncorrected. Elemental analyses were determined at the Microanalytical Laboratory of the College of Chemistry, University of California, Berkeley. X-ray structural determinations were performed at CHEXRAY, University of California, Berkeley.

The samples were prepared for X-ray absorption experiments as described previously, and the same methods were used to protect the air-sensitive compounds from oxygen and water.[16] X-ray absorption measurements were made at the Stanford Synchrotron Radiation Lightsource on beamline 11-2. The samples were prepared and loaded into a liquid-helium-flow cryostat at the beamline as described previously.[16] Data were collected at temperatures ranging from 30 to 300 K, using a Si(220) double-crystal monochromator. A linear extrapolation of the preedge absorption was subtracted, and the data were roughly normalized to unity above the edge. Energy calibration was performed by setting the peak in the first derivative of the absorption from a CeO_2 sample to 5724.0 eV. Fit methods were the same as described previously,[16,17] but are detailed in the SI, as well as Figure 5, showing that the individual fits and any remaining fit parameters not presented here. CeO_2 was purchased from commercial suppliers and used without further purification.

Magnetism. Magnetic susceptibility measurements were made for all samples in a 7 T Quantum Design Magnetic Properties Measurement System that utilizes a superconducting quantum interference device (SQUID). Sample containment and other experimental details have been described previously.[60] Diamagnetic corrections were made using Pascal's constants.[61]

In contrast to some of our previous work,[9,10,16,17] the combination of small magnetic signals and smaller quantities of the compounds made the container correction more critical for determining the TIP contribution, χ_0, for these data. Our primary method for containing samples for SQUID measurements is to sandwich them between pieces of quartz wool (as little as a few milligrams or as much as 20 mg) in a quartz tube. We consequently performed multiple measurements of quartz wool batches. It is important to note that quartz wool can have organic material on it from the manufacturing process and that we routinely bake the wool above 200 °C. However, we found that leaving the wool in an open beaker in an oven sometimes results in a higher magnetic impurity, possibly from trace amounts of iron oxide. We determined from our measurements that $\chi_0 = (-3.7 \pm 0.5) \times 10^{-7}$ emu/g for quartz wool, consistent with the value obtained for covalently bonded SiO_2 using a Pascal constant of -3.69×10^{-7} emu/g.[61] The estimated 13.5% error in the magnitude of the quartz wool correction in the data in Figures 3 and 4 gives the dominant error source in the estimate of χ_0 of the reported materials.

Another important correction is to remove any ferromagnetic impurity contribution by collecting data at multiple applied magnetic fields. The magnetic susceptibility is more rigorously defined as $\chi = dM/dH$, where M is the measured magnetism and H is the applied field, rather than the more common use of M/H. Here, we define $\chi = (M_2 - M_1)/(H_2 - H_1)$, where the subscript indicates measurements at two fields. This definition differs from the M/H estimate in the presence of a magnetic impurity, M_{imp}, and assumes a linear M versus H curve with a constant impurity contribution. M_{imp} can be estimated from the y intercept of M versus H, $M_{imp} = M_2 - \chi H_2$. It is important when using this correction to choose fields H_1 and H_2 to be large enough to saturate M_{imp} so that it can be treated as a constant, which is typically above 600 Oe. The data reported here were collected at 0.5 and 40 kOe. The exception is the data for CeO_2, which used a polycarbonate capsule container and was collected only at 1 kOe.

Synthesis. $Ce(acac)_4$ (1.00 g, 1.86 mmol) was added to a 250 mL round-bottomed Schlenk flask with 50 mL of toluene to yield a dark-red-brown solution. Sublimed trop (1.16 g, 8.2 mmol) was added to the flask, and this led to the immediate precipitation of a dark solid. The mixture was stirred for 1 h at room temperature and filtered to yield a dark-brown powder that was dried under reduced pressure to yield $Ce(trop)_4$ (935 mg, 80%). The dark-brown powder was recrystallized using Soxhlet extraction in CH_3Cl over 7 days to yield a dark-brown solution that was slowly evaporated to form a dark crystalline material, which was washed with pentane and dried under reduced pressure. $Ce(trop)_4$ is dark purple and insoluble in hydrocarbons and is only sparingly soluble in CH_2CH_2 or $CHCl_3$. An X-ray-suitable crystal was obtained by mixing a solution of $Ce(acac)_4$ and excess tropH in a a 10:2 $CHCl_3$/toluene solution. The resulting solution was allowed to slowly evaporate to form an X-ray-suitable crystal of $Ce(trop)_4$·tropH. ^{1}H NMR ($CDCl_3$, 400 MHz): δ 6.90 (t, 4H, J = 9.6 Hz), 7.08 (d, 8H, J = 10.8 Hz), 7.44 (t, 8H, J = 10.4 Hz). UV−vis [λ, nm (ε, cm^{-1} M^{-1})]: 238 (78200), 326 (44670), 366 (18500), 388 (6415), 460 (1500). Anal. Calcd for $C_{28}H_{20}O_8Ce$: C, 53.80; H, 3.23. Found: C, 53.51; H, 3.55. IR (cm^{-1}): 1590 (m), 1514 (s), 1425 (s), 1414 (s), 1365 (s), 1355 (s), 1248 (w), 1226 (m), 1219 (w), 1169 (w), 969 (w), 920 (w), 873 (w), 730 (m), 705 (w).

ASSOCIATED CONTENT

Supporting Information

The Supporting Information is available free of charge on the ACS Publications website at DOI: 10.1021/acs.inorgchem.8b00928.

Crystal data, tables, and ORTEP diagrams for $Ce(trop)_4$·tropH (PDF)

DOI: 10.1021/acs.inorgchem.8b00928
Inorg. Chem. 2018, 57, 7290−7298

Accession Codes

CCDC 1834248 contains the supplementary crystallographic data for this paper. These data can be obtained free of charge via www.ccdc.cam.ac.uk/data_request/cif, or by emailing data_request@ccdc.cam.ac.uk, or by contacting The Cambridge Crystallographic Data Centre, 12 Union Road, Cambridge CB2 1EZ, UK; fax: +44 1223 336033.

AUTHOR INFORMATION

Corresponding Authors

*E-mail: greg.nocton@polytechnique.edu (G.N.).
*E-mail: raandersen@lbl.gov (R.A.A.).

ORCID

Grégory Nocton: 0000-0003-0599-1176
Laurent Maron: 0000-0003-2653-8557

Notes

The authors declare no competing financial interest.

ACKNOWLEDGMENTS

G.N. thanks the CNRS and Ecole Polytechnique for funding. Dr. Thibault Cheisson is thanked for his help with determination of the shape parameters of $Ce(trop)_4$ and $Ce(tmtaa)_2$. Work at the University of California, Berkeley, and at Lawrence Berkeley National Laboratory was supported by the Director, Office of Energy Research, Office of Basic Energy Sciences, Chemical Sciences, Geosciences and Biosciences Division, Heavy Element Chemistry Program, of the U.S. Department of Energy under Contract DE-AC02-05CH11231. Use of the Stanford Synchrotron Radiation Lightsource, SLAC National Accelerator Laboratory, is supported by the U.S. Department of Energy, Office of Science, Office of Basic Energy Sciences, under Contract DE-AC02-76SF00515. L.M. is a member of the Institut Universitaire de France. Cines and CALMIP are acknowledged for a generous grant of computing time. L.M. also thanks the Humboldt Foundation for a fellowship.

REFERENCES

(1) Forsberg, B. D. *Gmelin Handbuch der Anorganischen Chemie*; Springer: Berlin, 1981; Vol. *D-3*, pp 54−247.
(2) Neumann, C. S.; Fulde, P. Is There a Molecular Analog of a Kondo Singlet-State. *Z. Phys. B: Condens. Matter* **1989**, *74* (3), 277−278.
(3) Dolg, M.; Fulde, P.; Kuchle, W.; Neumann, C. S.; Stoll, H. Ground-State Calculations of Di-Pi-Cyclooctatetraene Cerium. *J. Chem. Phys.* **1991**, *94* (4), 3011−3017.
(4) Dolg, M.; Fulde, P.; Stoll, H.; Preuss, H.; Chang, A.; Pitzer, R. M. Formally Tetravalent Cerium and Thorium Compounds - a Configuration-Interaction Study of Cerocene $Ce(C_8h_8)_2$ and Thorocene $Th(C_8h_8)_2$ Using Energy-Adjusted Quasi-Relativistic Ab-Initio Pseudopotentials. *Chem. Phys.* **1995**, *195* (1−3), 71−82.
(5) Dolg, M.; Fulde, P. Relativistic and Electron-Correlation Effects in the Ground States of Lanthanocenes and Actinocenes. *Chem. - Eur. J.* **1998**, *4* (2), 200−204.
(6) Kerridge, A. Oxidation state and covalency in f-element metallocenes (M = Ce, Th, Pu): a combined CASSCF and topological study. *Dalton Trans.* **2013**, *42* (46), 16428−16436.
(7) Kerridge, A.; Coates, R.; Kaltsoyannis, N. Is Cerocene Really a Ce(III) Compound? All-Electron Spin−Orbit Coupled CASPT2 Calculations on M(η8-C8H8)2 (M = Th, Pa, Ce). *J. Phys. Chem. A* **2009**, *113* (12), 2896−2905.
(8) Moosen, O.; Dolg, M. Two interpretations of the cerocene electronic ground state. *Chem. Phys. Lett.* **2014**, *594*, 47−50.
(9) Booth, C. H.; Walter, M. D.; Daniel, M.; Lukens, W. W.; Andersen, R. A. Self-contained Kondo effect in single molecules. *Phys. Rev. Lett.* **2005**, *95* (26), 267202.
(10) Walter, M. D.; Booth, C. H.; Lukens, W. W.; Andersen, R. A. Cerocene Revisited: The Electronic Structure of and Interconversion Between $Ce_2(C_8H_8)_3$ and $Ce(C_8H_8)_2$. *Organometallics* **2009**, *28* (3), 698.
(11) Lukens, W. W.; Walter, M. D. Quantifying Exchange Coupling in f-Ion Pairs Using the Diamagnetic Substitution Method. *Inorg. Chem.* **2010**, *49* (10), 4458−4465.
(12) Ashley, A.; Balazs, G.; Cowley, A.; Green, J.; Booth, C. H.; O'Hare, D. Bis(permethylpentalene)cerium - another ambiguity in lanthanide oxidation state. *Chem. Commun.* **2007**, *15*, 1515−1517.
(13) Balazs, G.; Cloke, F. G. N.; Green, J. C.; Harker, R. M.; Harrison, A.; Hitchcock, P. B.; Jardine, C. N.; Walton, R. Cerium(III) and Cerium(IV) Bis(η^8-pentalene) Sandwich Complexes: Synthetic, Structural, Spectroscopic, and Theoretical Studies. *Organometallics* **2007**, *26* (13), 3111−3119.
(14) Coreno, M.; de Simone, M.; Green, J. C.; Kaltsoyannis, N.; Narband, N.; Sella, A. Photoelectron spectroscopy of Ce(η-C5H5)3 − Accessing two ion states on 4f ionization. *Chem. Phys. Lett.* **2006**, *432* (1−3), 17−21.
(15) Denning, R. G.; Harmer, J.; Green, J. C.; Irwin, M. Covalency in the 4f Shell of tris-Cyclopentadienyl Ytterbium ($YbCp_3$)-A Spectroscopic Evaluation. *J. Am. Chem. Soc.* **2011**, *133* (50), 20644−20660.
(16) Booth, C. H.; Walter, M. D.; Kazhdan, D.; Hu, Y.-J.; Lukens, W. W.; Bauer, E. D.; Maron, L.; Eisenstein, O.; Andersen, R. A. Decamethylytterbocene Complexes of Bipyridines and Diazabutadienes: Multiconfigurational Ground States and Open-Shell Singlet Formation. *J. Am. Chem. Soc.* **2009**, *131* (18), 6480−6491.
(17) Booth, C. H.; Kazhdan, D.; Werkema, E. L.; Walter, M. D.; Lukens, W. W.; Bauer, E. D.; Hu, Y.-J.; Maron, L.; Eisenstein, O.; Head-Gordon, M.; Andersen, R. A. Intermediate-Valence Tautomerism in Decamethylytterbocene Complexes of Methyl-Substituted Bipyridines. *J. Am. Chem. Soc.* **2010**, *132* (49), 17537−17549.
(18) Nocton, G.; Booth, C. H.; Maron, L.; Andersen, R. A. Thermal Dihydrogen Elimination from Cp*2Yb(4,5-diazafluorene). *Organometallics* **2013**, *32* (5), 1150−1158.
(19) Nocton, G.; Booth, C. H.; Maron, L.; Andersen, R. A. Influence of the Torsion Angle in 3,3′-Dimethyl-2,2′-bipyridine on the Intermediate Valence of Yb in $(C_5Me_5)2Yb(3,3'\text{-}Me_2\text{-bipy})$. *Organometallics* **2013**, *32* (19), 5305−5312.
(20) Nocton, G.; Booth, C. H.; Maron, L.; Ricard, L.; Andersen, R. A. Carbon−Hydrogen Bond Breaking and Making in the Open-Shell Singlet Molecule $Cp^*_2Yb(4,7\text{-}Me_2phen)$. *Organometallics* **2014**, *33*, 6819−6829.
(21) Nocton, G.; Lukens, W. L.; Booth, C. H.; Rozenel, S. S.; Medling, S. A.; Maron, L.; Andersen, R. A. Reversible Sigma C−C Bond Formation Between Phenanthroline Ligands Activated by $(C_5Me_5)_2Yb$. *J. Am. Chem. Soc.* **2014**, *136* (24), 8626−8641.
(22) Goudy, V.; Jaoul, A.; Cordier, M.; Clavaguéra, C.; Nocton, G. Tuning the Stability of Pd(IV) Intermediates Using a Redox Noninnocent Ligand Combined with an Organolanthanide Fragment. *J. Am. Chem. Soc.* **2017**, *139* (31), 10633−10636.
(23) Isago, H.; Shimoda, M. Mixed Valence State of Cerium in Bis(phthalocyaninato)cerium Complex. *Chem. Lett.* **1992**, *21* (1), 147−150.
(24) Bian, Y.; Jiang, J.; Tao, Y.; Choi, M. T. M.; Li, R.; Ng, A. C. H.; Zhu, P.; Pan, N.; Sun, X.; Arnold, D. P.; Zhou, Z.-Y.; Li, H.-W.; Mak, T. C. W.; Ng, D. K. P. Tuning the Valence of the Cerium Center in (Na)phthalocyaninato and Porphyrinato Cerium Double-Deckers by Changing the Nature of the Tetrapyrrole Ligands. *J. Am. Chem. Soc.* **2003**, *125* (40), 12257−12267.
(25) Walter, M. D.; Fandos, R.; Andersen, R. A. Synthesis and magnetic properties of cerium macrocyclic complexes with tetramethyldibenzotetraaza[14]annulene, tmtaaH(2). *New J. Chem.* **2006**, *30* (7), 1065−1070.

DOI: 10.1021/acs.inorgchem.8b00928
Inorg. Chem. 2018, 57, 7290−7298

(26) Muetterties, E. L.; Wright, C. M. Chelate Chemistry. III. Chelates of High Coordination Number. *J. Am. Chem. Soc.* **1965**, *87* (21), 4706−4717.
(27) Campbell, D. L.; Moeller, T. Observations on the rare earths MLXXXI formation constants of tropolone chelates of the tripositive ions at 25°. *J. Inorg. Nucl. Chem.* **1969**, *31* (4), 1077−1082.
(28) Stary, J.; Liljenzin, J. O. Critical evaluation of equilibrium constants involving acetylacetone and its metal chelates. *Pure Appl. Chem.* **1982**, *54* (12), 2557−2592.
(29) Dorfner, W. L.; Carroll, P. J.; Schelter, E. J. A homoleptic eta(2) hydroxylaminato Ce-IV complex with S-4 symmetry. *Dalton Trans.* **2014**, *43* (17), 6300−6303.
(30) Bogart, J. A.; Lewis, A. J.; Boreen, M. A.; Lee, H. B.; Medling, S. A.; Carroll, P. J.; Booth, C. H.; Schelter, E. J. A Ligand Field Series for the 4f-Block from Experimental and DFT Computed Ce(IV/III) Electrochemical Potentials. *Inorg. Chem.* **2015**, *54* (6), 2830−2837.
(31) Bogart, J. A.; Lewis, A. J.; Medling, S. A.; Piro, N. A.; Carroll, P. J.; Booth, C. H.; Schelter, E. J. Homoleptic Cerium(III) and Cerium(IV) Nitroxide Complexes: Significant Stabilization of the 4+Oxidation State. *Inorg. Chem.* **2013**, *52* (19), 11600−11607.
(32) Matkovic, B.; Grdenic, D. The crystal structure of cerium(IV) acetylacetonate. *Acta Crystallogr.* **1963**, *16* (6), 456−461.
(33) Titze, H.; et al. Crystal structure of the beta-tetrakis-(acetylacetonato)cerium(4). *Acta Chem. Scand.* **1969**, *23* (2), 399−408.
(34) Titze, H.; et al. Crystal structure of the alfa-tetrakis-(acetylacetonato)cerium(IV). *Acta Chem. Scand.* **1974**, *28A* (10), 1079−1088.
(35) Behrsing, T.; Bond, A. M.; Deacon, G. B.; Forsyth, C. M.; Forsyth, M.; Kamble, K. J.; Skelton, B. W.; White, A. H. Cerium acetylacetonates - new aspects, including the lamellar clathrate Ce(acac)(4) center dot 10H(2)O. *Inorg. Chim. Acta* **2003**, *352*, 229−237.
(36) Becht, M.; Dahmen, K. H.; Gramlich, V.; Marteletti, A. Crystal structure and thermal behavior of some cerium complexes with the fluorinated β-diketonate ligand 6,6,6-trifluoro-2,2-dimethyl-3,5-hexanedione (fdh). *Inorg. Chim. Acta* **1996**, *248* (1), 27−33.
(37) Baxter, I.; Darr, J. A.; Hursthouse, M. B.; Malik, K. M. A.; Mingos, D. M. P.; Plakatouras, J. C. Preparation and crystal structures of the Ce(IV) β-diketonates, [Ce(tmhd)$_4$] and [Ce(pmhd)$_4$] (tmhd = 2,2,6,6-tetramethylheptane-3,5-dionate and pmhd = 1-phenyl-5-methylhexane-1,3-dionate). *J. Chem. Crystallogr.* **1998**, *28* (4), 267−276.
(38) Stilinović, V.; Kaitner, B. Two tetrakis(benzoylacetonato)-lanthanide species: synthesis, characterization and structures of tetrakis(benzoylacetonato)cerium(IV) and triethylammonium tetrakis-(benzoylacetonato)lanthanate(III) tetrahydrate. *J. Coord. Chem.* **2009**, *62* (16), 2698−2708.
(39) Leskela, M.; Sillanpaa, R.; Niinisto, L.; Tiitta, M.; Sjöström, M.; Wold, S.; Berglind, R.; Karlsson, B. Structural and Thermal Studies of Tetrakis(2,2,6,6-tetramethyl-3,5-heptanedionato)cerium(IV). *Acta Chem. Scand.* **1991**, *45*, 1006.
(40) Gottfriedsen, J.; Hagner, R.; Spoida, M.; Suchorski, Y. Synthesis, Structure, and Reactivity of Cerium(IV) Calix[4]arene Complexes. *Eur. J. Inorg. Chem.* **2007**, *2007* (16), 2288−2295.
(41) DelaRosa, M.; Bousman, K.; Welch, J.; Toscano, P. Physical and Structural Characterization of Ce(IV) β-Diketonate Complexes: Evidence for Geometrical Isomers in the Solid-State. *J. Coord. Chem.* **2002**, *55* (7), 781−793.
(42) Kepert, D. L.; Patrick, J. M.; White, A. H. Structure and stereochemistry in f-block complexes of high co-ordination number. Part 4. The [M(bidentate ligand)4] system: crystal structures of tetrakis(dibenzoylmethanato)-uranium(IV) and -cerium(IV). *J. Chem. Soc., Dalton Trans.* **1983**, No. 3, 567−570.
(43) Troyanov, S. I.; Moroz, S. A.; Snezhko, N. I. *Koord. Khim.* **1992**, *18*, 1207.
(44) Zhang, J.; Badger, P. D.; Geib, S. J.; Petoud, S. Synthesis and Structural Properties of Lanthanide Complexes Formed with Tropolonate Ligands. *Inorg. Chem.* **2007**, *46* (16), 6473−6482.
(45) Davis, A. R.; Einstein, F. W. B. The crystal and molecular structure of tetrakis(tropolonato)zirconium(IV) chloroform: Zr-(C7H5O2)4. (CHCl3)2.25. *Acta Crystallogr., Sect. B: Struct. Crystallogr. Cryst. Chem.* **1978**, *34* (7), 2110−2115.
(46) Tranqui, D.; Tissier, A.; Laugier, J.; Boyer, P. Structure cristalline du complexe moleculaire HfT4-DMF (tropolonate de hafnium-N,N-dimethylformamide). *Acta Crystallogr., Sect. B: Struct. Crystallogr. Cryst. Chem.* **1977**, *33* (2), 392−397.
(47) Nomiya, K.; Onodera, K.; Tsukagoshi, K.; Shimada, K.; Yoshizawa, A.; Itoyanagi, T.-a.; Sugie, A.; Tsuruta, S.; Sato, R.; Kasuga, N. C. Syntheses, structures and antimicrobial activities of various metal complexes of hinokitiol. *Inorg. Chim. Acta* **2009**, *362* (1), 43−55.
(48) Davis, A. R.; Einstein, F. W. B. Eight-coordination and hydrogen bonding in a complex of scandium. Crystal structure of the acid dimer of tetrakis(tropolonato)scandium(III). *Inorg. Chem.* **1974**, *13* (8), 1880−1884.
(49) Anderson, T. J.; Neuman, M. A.; Melson, G. A. Coordination chemistry of scandium. VII. Crystal and molecular structure of hydrogentetrakis(tropolonato)scandium(III), a scandium(III) complex with approximate D2d dodecahedral stereochemistry. *Inorg. Chem.* **1974**, *13* (8), 1884−1890.
(50) Muetterties, E. L.; Guggenberger, L. J. Idealized polytopal forms. Description of real molecules referenced to idealized polygons or polyhedra in geometric reaction path form. *J. Am. Chem. Soc.* **1974**, *96* (6), 1748−1756.
(51) Steffen, W. L.; Fay, R. C. Reinvestigation of the coordination geometry of eight-coordinate metal tetrakis(acetylacetonates). *Inorg. Chem.* **1978**, *17* (3), 779−782.
(52) Davis, A. R.; Einstein, F. W. B. Factors affecting the shape of eight-coordinate species. Crystal and molecular structure of (NbT4)-2(O(H···Cl)3)(.CH3CN). *Inorg. Chem.* **1975**, *14* (12), 3030−3035.
(53) Kotani, A.; Kvashnina, K. O.; Butorin, S. M.; Glatzel, P. A new method of directly determining the core−hole effect in the Ce L_3 XAS of mixed valence Ce compounds—An application of resonant X-ray emission spectroscopy. *J. Electron Spectrosc. Relat. Phenom.* **2011**, *184* (3), 210−215.
(54) Minasian, S. G.; Batista, E. R.; Booth, C. H.; Clark, D. L.; Keith, J. M.; Kozimor, S. A.; Lukens, W. W.; Martin, R. L.; Shuh, D. K.; Stieber, S. C. E.; Tylisczcak, T.; Wen, X.-d. Quantitative Evidence for Lanthanide-Oxygen Orbital Mixing in CeO_2, PrO_2, and TbO_2. *J. Am. Chem. Soc.* **2017**, *139* (49), 18052−18064.
(55) Keski-Rahkonen, O.; Krause, M. O. Total and partial atomic-level widths. *At. Data Nucl. Data Tables* **1974**, *14* (2), 139−146.
(56) Van Vleck, J. H. *The Theory of Electric and Magnetic Susceptibilities*; Oxford University Press: London, 1932.
(57) Orchard, A. F. *Magnetochemistry*; Oxford University Press: Oxford, 2003.
(58) Ganduglia-Pirovano, M. V.; Hofmann, A.; Sauer, J. Oxygen vacancies in transition metal and rare earth oxides: Current state of understanding and remaining challenges. *Surf. Sci. Rep.* **2007**, *62* (6), 219−270.
(59) Pinnavaia, T. J.; Fay, R. C.; Fackler, J. P.; Fetchin, J.; Seidel, W. Tetrakis(2,4-pentanedionato)cerium(IV) and Tetrakis(1,1,1-trifluoro-2,4-pentanedionato)cerium(IV). *Inorganic Syntheses*; John Wiley & Sons, Inc., 2007; pp 77−80.
(60) Walter, M. D.; Schultz, M.; Andersen, R. A. Weak paramagnetism in compounds of the type CP ' Yb-2(bipy). *New J. Chem.* **2006**, *30* (2), 238−246.
(61) Bain, G. A.; Berry, J. F. Diamagnetic corrections and Pascal's constants. *J. Chem. Educ.* **2008**, *85* (4), 532−536.

DOI: 10.1021/acs.inorgchem.8b00928
Inorg. Chem. 2018, 57, 7290−7298